CozEa and CozEb play overlapping and essential roles in controlling cell division in *Staphylococcus aureus*

Gro Anita Stamsås[1¶], Ine Myrbråten[1¶], Daniel Straume[1], Zhian Salehian[1], Jan-Willem Veening[2], Leiv Sigve Håvarstein[1], Morten Kjos[1*]

[1] Faculty of Chemistry, Biotechnology and Food Science, Norwegian University of Life Sciences, Ås, Norway.

[2] Department of Fundamental Microbiology, Faculty of Biology and Medicine, University of Lausanne, Lausanne, Switzerland.

[*] Corresponding author

E-mail: morten.kjos@nmbu.no (MK)

[¶] These authors contributed equally to this work.

Abstract

Staphylococcus aureus needs to tightly control the position and timing of cell division and cell wall synthesis to maintain its spherical shape. It is largely unknown which factors that contribute to this control. In oval-shaped *Streptococcus pneumoniae*, $CozE^{Spn}$, was recently identified as a protein controlling the timing of cell elongation. The spherical coccus *S. aureus* has two homologs of $CozE^{Spn}$, here named CozEa and CozEb. *cozEa* or *cozEb* could be deleted without major growth or morphological defects. However, the Δ*cozEa*Δ*cozEb* double mutant could not be made. To study the functions of *cozEa* and *cozEb*, we constructed a dCas9-based CRISPR interference (CRISPRi) system for *S. aureus*, allowing knockdown of expression of essential genes. Using our novel CRISPRi system, we show that *cozEa* and *cozEb* have essential and overlapping functions in *S. aureus*: depletion of *cozEa* in the Δ*cozEb* strain (and vice versa) causes severe morphological defects with uncoordinated timing and positioning of cell division as well as aberrant nucleoid morphologies. Using two-hybrid interaction assays, we found that both CozEa and CozEb could interact with the early cell division protein EzrA. Notably, we find that the interaction between CozE and EzrA is conserved, and we show that also in *S. pneumoniae*, cell division is mislocalized in $cozE^{Spn}$-depleted cells. Finally, we demonstrate that both CozEa and CozEb could complement deletion of *cozE* in *S. pneumoniae*, further suggesting that the functions of these proteins are at least partially conserved. Together, our results show that CozE proteins mediate control of cell division in *S. aureus* and *S. pneumoniae*, likely via interactions with key cell division proteins such as EzrA.

Introduction

Bacterial cell division initiates when the tubulin-like protein FtsZ polymerizes into a ring structure (Z-ring) located at the future division site. The Z-ring then serves as a scaffold for recruitment of cell division and cell wall synthesis proteins, forming the multiprotein complex known as the divisome. Several of the proteins constituting the divisome are widely conserved in most bacteria, while others are specific for bacterial subgroups or have diverged significantly [1]. Positioning and timing of Z-ring assembly and cell wall synthesis are dependent on the shape of the bacterium; and there are large variations between coccal, ovococcal and rod-shaped bacteria.

Staphylococcus aureus often serves as the model organism for cell division studies in spherical bacteria. *S. aureus* is an opportunistic pathogen, which persistently colonizes around 20 % of the human population [2], causing both superficial infections on the skin and invasive, life-threatening sepsis as well as endocarditis in humans [3, 4]. Furthermore, *S. aureus* is an important pathogen among livestock (causing mastitis and other infections) and is a problematic food pathogen. Treatment of *S. aureus* infections with antibiotics is increasingly challenging due to the rise of antibiotic resistant strains, including MRSA (methicillin-resistant *S. aureus* which are resistant to β-lactam antibiotics) and VRSA (vancomycin-resistant *S. aureus*).

Cell division in spherical *S. aureus* occurs in three consecutive planes, where every new round of division is orthogonal to the previous division plane [1]. During the cell cycle, *S. aureus* cells gradually increase their volumes by slight elongation and the cross-wall is synthesized before the actual separation of daughter cells occurs on a timescale of milliseconds [5, 6]. Many key cell division proteins known from other model bacteria are conserved in *S. aureus*, including FtsZ, FtsA, EzrA, GpsB, DivIB, DivIC, DivIVA, MreC and MreD [1, 7-10]. Most of these proteins are in different ways involved in formation of the division ring and for ensuring proper cell wall synthesis. For example, EzrA is a key protein linking division ring formation and the cell wall synthesis machinery [9, 11]. Cell wall synthesis in *S. aureus* takes place at midcell, where new peptidoglycan units are incorporated into the cell wall by transglycosylation (PBP2) and transpeptidation reactions (PBP1, PBP2, PBP3 and PBP4). During each cell cycle, peptidoglycan synthesis and cell division need to be coordinated with DNA replication

and chromosome segregation. This is to ensure correct cell size homeostasis and that the two daughter cells each get one copy of the chromosome in time before the cell splits. Misregulation would result in daughter cells of variable sizes without DNA or guillotining of the chromosome by the septal cross-wall. How the timing and localization of Z-ring assembly and cell wall synthesis are regulated in *S. aureus*, given the geometry of cell division in three consecutive perpendicular planes, is still an unanswered question. One protein involved in this coordination is probably Noc (nucleoid occlusion protein) which both controls DNA replication [12] and inhibits Z-ring formation across the nucleoid [13]. Recent results also predict the protein DivIVA to have an important role in linking chromosome segregation to cell division [14].

The important human pathogen *S. pneumoniae* is an ovococcal bacterium, in which both septal (division) and peripheral (elongation) cell wall synthesis occur in the mid-cell area [15]. In these cells, positioning of the Z-ring at mid-cell has been shown to depend on several factors, including the chromosomal origin of replication [16] and the peptidoglycan binding protein MapZ [17, 18]. Most likely, the septal and peripheral cell wall growth in pneumococcal cells are mediated by separate protein machineries, whose actions are tuned by different regulatory proteins such as StkP, GpsB, DivIVA or EloR [15, 19-24]. Another protein involved in regulation of cell wall synthesis in pneumococci, named CozE (for coordinator of zonal elongation, SPD_0768 in strain D39 and Spr0777 in strain R6), was recently identified [21, 25]. CozE, a multi-transmembrane spanning protein, was found to be essential for normal growth, however, it's essentiality was abolished in the absence of the bifunctional penicillin-binding protein PBP1a or the cell wall elongation proteins MreC and MreD [25]. In protein-protein interaction assays, CozE was found to be associated with the same proteins (PBP1a, MreC, MreD) as well as DivIVA and PBP2b [21, 25]. CozE was thus proposed to be a key regulator of cell elongation in *S. pneumoniae* by positioning PBP1a via interactions with MreC and MreD [15, 25]. CozE proteins are widespread among different bacteria [25]. Here we studied the two homologs of CozE in spherical *S. aureus* cells. We show that the CozE proteins are involved in coordinating cell division in *S. aureus* and that this function is conserved also in *S. pneumoniae*.

Results

The two CozE homologs of *S. aureus*

The protein CozE (for coordinator of zonal elongation) was recently identified as an essential cell division protein in oval shaped pneumococcal cells, where it has been shown to be involved in regulation of proper cell elongation [21, 25]. Spherical *S. aureus* does not elongate to the same extent as *S. pneumoniae* and other rod- or oval-shaped bacteria [1]. Nevertheless, homology searches showed that *S. aureus* encodes two proteins homologous to CozE, and we therefore set out to unravel the function of CozE in these spherical cells. Sequence comparison of the pneumococcal CozE (hereafter $CozE^{Spn}$) with the two CozE-homologs of *S. aureus* SH1000, SAOUHSC_00948 (hereafter CozEa) and SAOUHSC_01358 (hereafter CozEb), shows that they are 31 % and 30 % identical to $CozE^{Spn}$, respectively (Fig S1). When compared with each other, CozEa and CozEb are 30 % identical. The *cozEa* gene is predicted to be monocistronic, while *cozEb* is located as the last open reading frame on a three-gene operon which also encodes a transcription antiterminator (*glcT*) and a small, putative membrane spanning protein (SAOUCHSC_01357) (Fig 1A).

Using the temperature sensitive vector pMAD [26], *cozEa* and *cozEb* were deleted individually in *S. aureus* SH1000 by allelic exchange with a spectinomycin resistance cassette. The deletion mutants SAMK24 (Δ*cozEa*::*spc*) and SAMK21 (Δ*cozEb*::*spc*) did not exhibit any growth defect compared to wild-type (Fig 1B). Analysis of cell sizes showed that the cell diameter of both mutants, on average, are slightly smaller compared to the wild-type (Fig 1C and D). No obvious differences in cell wall labelling (using fluorescent vancomycin, VanFL) or nucleoid staining patterns (using DAPI) were observed between the mutants and wild-type (Fig 1C).

In order to see whether the two mutant strains, SAMK21 and SAMK22, had acquired any suppressor mutations elsewhere in the genome, we resequenced their genomes and compared it to the SH1000 wild-type genome. SAMK24 did not contain any additional mutations. In SAMK21, a single conservative SNP was found in the gene *thiI* (SAOUHSC_01824) encoding a probable tRNA sulphurtransferase. This SNP (A970T) resulted in a conservative substitution of isoleucine with a phenylalanine (I324F). Our later experiments (see below) show that this mutation is not important for

the functionality of *cozEb* (or *cozEa*) and we therefore conclude that neither CozEa nor CozEb are essential for normal growth and cell division in *S. aureus* SH1000.

Single deletions of *cozEa* or *cozEb* both cause a small reduction in cell size. To investigate the effects of a double deletion, another pMAD deletion vector (pMAD-*cozEa*::*cam*) was constructed to delete *cozEa* in the Δ*cozEb*::*spc* background. However, despite multiple attempts, we were unable to obtain the double deletion strain. This suggests that *cozEa* and *cozEb* may have complementary and essential functions.

Construction of a two-plasmid CRISPR interference system for *S. aureus*

Since double deletions of *cozEa* and *cozEb* could not be obtained, we instead wanted to study the phenotypes of the cells when *cozEa* or *cozEb* gene expression was knocked down in Δ*cozEb* or Δ*cozEa* background, respectively. We therefore constructed a CRISPR/dCas9 knockdown system to allow inducible depletion of essential genes. The CRISPR interference systems developed for *S. pneumoniae* and *Bacillus subtilis* [27, 28] were used as models. A catalytically inactive Cas9 (dead Cas9, dCas9) was cloned downstream of an IPTG-inducible promoter in the low-copy number plasmid pLOW (pSK41 minireplicon, Fig 2A) [29]. A single guide RNA (sgRNA) construct, consisting of a 20 nt base-pairing region and a Cas9-handle region, was inserted downstream of a synthetic, constitutive promoter in the plasmid pCG248 (replicon T181, Fig 2A) [30]. Targeting of the gene of interest is accomplished by replacing the 20 nt sequence using inverse PCR as described in the Methods section. Notably, multi-sgRNA plasmids can be constructed by using the BglII and BamHI restriction sites located up- and downstream of the sgRNA construct, as outlined in Fig S2. A schematic view of the resulting two-plasmid CRISPRi system is shown in Fig 2A.

To quantify the efficiency of our CRISPRi system, we created a RN4220-derivative strain with constitutive expression of a monomeric superfolder GFP (*m(sf)gfp*), SAMK56, and designed an sgRNA targeting the *m(sf)gfp* gene. As shown in Fig 2B, GFP expression could be titrated by increasing the IPTG concentrations. Maximum depletion was obtained with ≥100 µM IPTG. To investigate how quick GFP expression was switched off after IPTG induction, SAMK56 was induced with 100 µM IPTG and

samples were taken every 30th min for 3 hrs. The GFP fluorescence levels (Fig 2C) decreased rapidly, suggesting that expression was switched off almost immediately. Furthermore, as a proof of the functionality of the CRISPRi system in targeting essential cell cycle genes, we created sgRNAs targeting the DNA replication initiator *dnaA* (encoded on an operon with *dnaN*) and *pbp1* (monocistronic) encoding a penicillin-binding protein. The CRISPRi strains were analyzed by growth assays and microscopy (Fig 2D-F), and the observed phenotypes were as expected, confirming the suitability of the CRISPRi system to study the function of essential genes; compared to the control strain (Fig 2D), the *pbp1* depletion resulted in clustered, larger cells with aberrant morphologies (Fig 2E) [31, 32] while *dnaA* depletion resulted in anucleate cells with variable sizes and nucleoid morphologies (Fig 2F).

CozEa and CozEb are synthetic lethal and important for proper cell cycle progression in *S. aureus*

We made sgRNA constructs targeting *cozEa* and *cozEb*, and depleted expression of *cozEa* in the Δ*cozEb* background and vice versa. Note that *cozEa* is monocistronic, while *cozEb* is located as the last gene in the operon, and the knockdown will therefore have minimal polar effects [27, 28]. No growth reduction was observed upon knockdown of the individual genes in wild-type background (as expected from the deletion mutants) (Fig 3A and B). On the other hand, in the deletion backgrounds, knockdown of the other gene was detrimental for growth (Fig 3A and B). Notably, the effect of knockdown is seen already without added inducer, reflecting that there is a leaky expression of dCas9 from the IPTG-inducible promoter in pLOW [29]. From this we conclude that *cozEa* and *cozEb* have essential, overlapping functions in *S. aureus*, as the absence of both genes is not tolerated.

The phenotypes of the GS1167 (Δ*cozEa*::*spc*, depleted *cozEb*) and GS1163 (Δ*cozEb*::*spc*, depleted *cozEa*) strains were then further investigated by microscopy. Phase contrast micrographs revealed severely perturbed cell morphologies when the CRISPRi system is induced, displaying both variable cell shapes and sizes as well as increased clustering of cells (Fig 4A). Measurements of the cell diameter of CRISPRi-induced GS1167 and GS1163 cells show that they have a very wide distribution

compared to the wild type (Fig 4B). We also made a double sgRNA strain allowing knockdown of both *cozEa* and *cozEb* simultaneously with the CRISPRi system (strain SAMK75), and as expected this strain displayed similar phenotype as the GS1167 and GS1163 strains (Fig S3).

Phase contrast micrographs of cells depleted of both *cozEa* and *cozEb* suggested that the septum was misplaced. This was further analyzed by transmission electron microscopy (TEM) (Fig 4C - D and Fig S4). GS1167 cells (Δ*cozEa*::spc with depleted *cozEb*) depleted for 4 hours developed striking incorrect and uncoordinated initiation of septum formation resulting in misshaped cells (Fig 4D). Empty, lysed cells were also observed (Fig 4D). In mildly depleted cells (depletion for 1 hour), the phenotype is less severe, however, uncoordinated initiation of septum formation and aberrant septa were also observed here (Fig S4). Electron micrographs of the individual deletions show that while no clear defect is observed in the Δ*cozEb* cells, Δ*cozEa* mutants do show mild morphological defects (Fig S4). In the latter case, lysed cells are also observed. Comparison of septum thickness based on the TEM images further show that the GS1167 on average has thicker septal cross-wall compared to wild-type cells. Furthermore, Δ*cozEb* has less thick septa than the Δ*cozEa* mutant (Fig S5).

Notably, nucleoid staining of the cells depleted of both *cozEa* and *cozEb* using DAPI was also abnormal with non-homogeneous staining patterns. A large fraction of the cells appeared to have high intensity or highly condensed DAPI signals (47.1 % for GS1167, 22.9 % for GS1163, n > 250) compared to the wild type, and some cells were also anucleate under these conditions (4.1 % for GS1167 and 2.0 % for GS1163, n > 250) (Fig 4A). The chromosome biology of the cells thus also seems to be perturbed when CozEa and CozEb are lacking.

CozEa and CozEb do not affect cell wall composition, but interact with key cell division proteins

TEM images showed that the septal cell wall appeared different between wild-type and the *cozE*-deficient cells; initiation of cell wall synthesis seems to be uncoordinated (Fig 4) and the septal cell wall is thicker in cells lacking *cozEa* (Fig S5). In *S. pneumoniae*, $CozE^{Spn}$ has been shown to interact with the bi-functional penicillin binding protein PBP1a [25]. To get insight into whether CozEa and CozEb

could influence cell wall synthesis, we first investigated whether these proteins could interact with any of the four PBPs of *S. aureus* (PBP 1, PBP 2, PBP3 and PBP4) using bacterial two-hybrid assays (see Material and Methods for detailed description) [33]. While CozEa and CozEb both self-interacted and interacted with each other, no interaction was found with any of the PBPs of *S. aureus* (Fig 5A). We also tested the methicillin-resistant PBP2a (MecA) from *S. aureus* COL, but we could not find any interactions with the CozE proteins (Fig 5A). Next, we analyzed the muropeptide composition of peptidoglycan derived from strain the GS1167 (Δ*cozEa* with depleted *cozEb*), to see whether the cell wall structure was altered in this mutant. However, the muropeptide composition of GS1167 was similar to the wild-type (Fig 5B). This suggests that CozEa and CozEb affect positioning and timing of cell division and cross-wall synthesis, but that the cell wall synthesis pathway is unaltered.

We further analyzed whether CozEa and CozEb could interact with a selection of other key cell cycle proteins using bacterial two-hybrid assays (Fig 5C, S1 Table). $CozE^{Spn}$ has been shown to interact with $MreC^{Spn}$, $MreD^{Spn}$ and $DivIVA^{Spn}$ [21, 25]. We detected an interaction between CozEa and MreC, however, this was not the case for CozEb. No interactions with MreD or DivIVA were observed for any of the combinations (Fig 5C, S1 Table). The only protein we could identify that interacted with both CozEa and CozEb was the early cell division protein EzrA. Among the other proteins tested, we also found that CozEa and GpsB interacted, however, not CozEb and GpsB. A full overview of all tested bacterial two-hybrid interactions are given in S1 Table.

The positive two-hybrid interactions suggest that CozEa and CozEb may mediate cell division control via interactions with EzrA, but this hypothesis needs to be further tested. Interestingly, knockdown of *ezrA* using the CRISPRi system leads to similar phenotypes as cells lacking CozEa and CozEb (Fig 5D) with variable cell sizes. This is fully in line with previous results of *ezrA* deletions and knockdown mutants in *S. aureus* [9, 11]. Note that the cell size effect is observed also, but to a lesser extent, when no IPTG is added, again reflecting leaky expression from the P_{lac} promoter. Abnormal DAPI staining pattern was also observed in the cells after IPTG induction, although this phenotype appear to be less pronounced in the *ezrA* knockdown cells (5.5 % of cells, n = 200) compared to cells depleted of CozEa and CozEb. It should also be noted that the growth rate was not severely affected

upon induction of *ezrA* knockdown (Fig S6), suggesting that *ezrA* is not essential for normal growth under these conditions [10].

The division ring is mislocalized in *S. pneumoniae* cells depleted of CozE^{Spn}

The results above demonstrate that CozEa and CozEb play functionally overlapping roles in controlling cell division in *S. aureus*, but they are not essential alone. As mentioned above, a single protein CozE^{Spn} (SPD_0768 in strain D39 and Spr0777 in strain R6), is shown to be essential for growth and proper cell morphology in *S. pneumoniae* [21, 25]. To investigate whether the EzrA-interactions detected here were specific for *S. aureus* or also relevant in *S. pneumoniae*, we used bacterial two-hybrid assays to test the interaction between CozE^{Spn} and EzrA^{Spn}. Just like the staphylococcal proteins, a strong interaction was found between the corresponding pneumococcal proteins (Fig 6A). Strikingly, while EzrA localized to midcell in wild-type *S. pneumoniae* (Fig 6B and C), the protein is clearly mislocalized in cells where *cozE^{Spn}* was depleted (Fig 6D).

S. aureus cozE can complement the Δ*cozE^{Spn}* phenotype of *S. pneumoniae*

In order to gain further insight into functional conservation of CozE proteins between *S. aureus* and *S. pneumoniae*, we tested whether CozEa or CozEb could functionally complement the essential CozE^{Spn} in *S. pneumoniae*. We created pneumococcal strains in which *cozEa* and *cozEb* were chromosomally integrated downstream of the ComRS-inducible promoter, P_{comX}. Induction of P_{comX} is achieved by addition of the peptide ComS to the growth medium; ComS is internalized where it activates the P_{comX}-binding transcriptional activator ComR [34]. Next, we attempted to delete the native *cozE^{Spn}* by allelic exchange with the Janus cassette [35], with and without presence of the inducer ComS. A functional complementation with CozEa or CozEb in the pneumococcus would allow deletion of the *cozE*^{Spn} gene. Indeed, upon induction of *cozEa* or *cozEb* expression with 2 µM ComS, the native *cozE^{Spn}* could readily be deleted (Table 1). It should be noted that the CozEa and CozEb probably have a reduced functionality compared to CozE^{Spn}, as higher inducer concentrations were required to obtain correct transformants for the non-native CozE-proteins (Table 1). Additionally, CozEa seemed to function better than CozEb,

since the number of transformants were higher for the former. Microscopy of the resulting strains further confirmed that the typical *cozE*^{Spn}-depletion phenotype in pneumococci, characterized by extensive chaining and rounding of cells [21], could be complemented by CozEa or CozEb (Fig S7). Expression of either CozEa or CozEb restored the normal morphology of the CozE^{Spn} depleted cells (Fig S7).

Finally, to get insights into how the staphylococcal proteins CozEa and CozEb could complement CozE^{Spn}, we analyzed by bacterial two-hybrid assays whether CozEa and CozEb could still interact with EzrA^{Spn} (Fig 6A). Notably, both CozEa and CozEb interact with EzrA^{Spn} in this assay, with CozEa having stronger interaction than CozEb. Thus, conservation of the interaction with EzrA could thus explain why CozEa and CozEb were functional in *S. pneumoniae*.

Table 1. Complementation of *ΔcozE*^{Spn} in *S. pneumoniae* with CozEa and CozEb.

	Colonies/ml/ng[a]		
Complementation	**0 µM ComS**	**0.2 µM ComS**	**2 µM ComS**
P$_{comX}$-*cozE*^{Spn}	595 (0/8)[b]	>2000 (8/8)	>2000 (8/8)
P$_{comX}$-*cozEa*	65 (0/8)	580 (3/8)	>2000 (8/8)
P$_{comX}$-*cozEb*	71 (0/8)	77 (0/8)	45 (6/8)

[a] number of colonies on the plate after 16 hours (per 1 ml transformation mix per ng DNA) when the respective strains were transformed with the DNA fragment Δ*cozE*^{Spn}::P-*rpsL-kan* (Janus cassette). Transformants were selected with kanamycin. Eight colonies for each transformation were check by PCR, and the number of true Δ*cozE*^{Spn} verified by PCR per 8 colonies are indicated in brackets.

[b] When transforming with the Δ*cozE*^{Spn}::P-*rpsL-kan* cassette, small sized colonies are observed also without complementation. However, these are not true Δ*cozE*^{Spn} deletions when checked by PCR. In these colonies, *cozE*^{Spn} has moved to another chromosomal location (data not shown) and the strain has probably acquired suppressor mutations as previously observed.

Discussion

The membrane protein CozE^{Spn} was recently identified as an essential regulator of cell elongation in oval shaped *S. pneumoniae* [21, 25]. CozE proteins are widely conserved and present in the genome of bacteria from different phyla and of different morphologies [25]. We here show that the two CozE-homologs of *S. aureus*, which we named CozEa and CozEb, play overlapping roles to control proper cell cycle progression in these spherical cells.

While the deletion of either *cozEa* or *cozEb* has only minor effects, both genes cannot be deleted at the same time. To confirm the synthetic relationship between *cozEa* and *cozEb*, we developed a CRISPRi system for *S. aureus* to allow knockdown of expression of essential genes. Recent reports have already shown the suitability of using CRISPR/dCas9 for knockdown of genes in *S. aureus* [36, 37]. The plasmid-based CRISPR/dCas9-derived system we developed here contains several unique features compared to the published ones [36, 37]: (i) Knockdown is inducible by addition of IPTG, since dCas9 expression is driven by the IPTG-inducible promoter. (ii) The plasmid harbouring the sgRNA construct is relatively small (5.8 kb), thus allowing easy replacement of target sequences by inverse PCR. (iii) Multi-sgRNA plasmids, allowing simultaneous knockdown of several genes, can be constructed by combining existing sgRNA plasmids using BglBrick assembly [38] (Fig S2).

Using the CRISPRi system, we could construct combined deletion/depletion strains or double-depletion strains to study cells depleted of CozE proteins. Since all the different strains depleted of CozE proteins showed the same phenotypes, we could exclude that the conservative substitution in the gene *thiI* (detected by whole genome resequencing, see results) played any functional role. Low levels of CozEa and CozEb proteins have pleiotropic effects on the staphylococcal cells, including abnormal cell size homeostasis and nucleoid staining, frequent lysis, and, most strikingly, the lack of cell division coordination (Fig 4). Wild-type *S. aureus* cells divide in consecutive, perpendicular planes, ie. the new septum is formed perpendicular to the previous and splitting of daughter cells (popping) finishes before the next septum is formed [1, 5, 6]. In CozE-depleted cells, the coordination seems to be lacking: cells can initiate septum formation before the previous division cycle finishes and the two attached daughter

cells are not synchronized (Fig 4). Furthermore, non-perpendicular septa were also observed, resulting in elongated cells reminiscent of elongating staphylococcal FtsZ mutant strains [39].

Despite having misplaced and thicker septa than wild-type, the cell wall composition does not appear to be altered in the CozEa/CozEb-depleted cells and CozEa or CozEb are not directly interacting with any of the PBPs of *S. aureus*. An interaction between CozEa and MreC was detected, however, CozEa nor CozEb could interact with MreD. Also worth noting, MreC and MreD are non-essential in *S. aureus* [40]. The link between $CozE^{Spn}$ and the $MreCD^{Spn}$ complex to direct the action of PBPs and peptidoglycan synthesis as described by Fenton et al. [25] in *S. pneumoniae*, thus appear to be different in *S. aureus*.

Instead, we show that CozEa and CozEb could interact with one of the early cell division proteins, namely EzrA. The CozEa-EzrA and CozEb-EzrA interactions were found by testing a collection of proteins in a heterologous bacterial two-hybrid assay [33]. Thus, the *in vivo* relevance of this interaction needs to be verified further and there may also be important CozEa/CozEb interaction partners that we have not yet identified. Nevertheless, interaction with EzrA could be a plausible way for CozEa and CozEb to mediate cell division control. EzrA is one of the first proteins binding to the Z-ring in the initiation of cell division. EzrA was identified as a negative regulator of FtsZ formation in *B. subtilis* [41], and is thought to be important for the switch between elongation and division growth in *B. subtilis* via protein-protein interactions with penicillin-binding proteins [42]. In *S. aureus*, EzrA is involved in a large number of protein-protein interactions. Bacterial two-hybrid interactions have been shown between EzrA and FtsZ, DivIB, DivIC, FtsA, FtsL, Pbp1-3, SepF, GpsB, RodA [9] and DivIVA [14]. Although some of these interactions may be false positives, it clearly suggests that EzrA is a central protein for proper cell cycle progression in *S. aureus*. It has indeed been shown that EzrA plays a key role in staphylococcal cell size homeostasis; different levels of EzrA in the cells influence the cell size [9, 11]. We also observed the same when *ezrA* was targeted using the CRISPRi system (Fig 5). Furthermore, lack of EzrA causes mislocalization of other key cell division proteins such as FtsZ, GpsB and PBPs [9, 11]. Thus, disrupting the localization or functionality of EzrA, which may be the case in cells lacking CozEa and CozEb, will therefore likely have large pleiotropic effects on different cell cycle processes, and is consistent with the results of the current study. Note, however, that there are

conflicting results in the literature regarding the essentiality of ezrA [9, 11]. The results from our CRISPRi depletion suggest that *ezrA* is non-essential for growth under our experimental conditions. Thus, it is likely that CozEa/CozEb have other roles in *S. aureus* yet to be identified.

Our results also show that the influence of CozE on cell division observed in *S. aureus* was conserved in ovococcal *S. pneumoniae*. Just like in *S. aureus*, $CozE^{Spn}$ could interact with $EzrA^{Spn}$ in bacterial two-hybrid assays and depletion of $CozE^{Spn}$ in *S. pneumoniae* caused aberrant cell division placement as observed by mislocalization of $EzrA^{Spn}$-GFP. In line with this, $EzrA^{Spn}$ interacts with $FtsZ^{Spn}$, $GpsB^{Spn}$ and $DivIVA^{Spn}$ and is important for coordination of septal and peripheral cell wall synthesis in ovococcal *S. pneumoniae* cells [19, 20]. Depletion of $ezrA^{Spn}$ expression in *S. pneumoniae* (Fig 5) also resulted in cells with variable sizes and nucleoid staining pattern as well as multiple or misplaced septa [27]. Notably, both *cozEa* and *cozEb* could complement the $\Delta cozE^{Spn}$ in *S. pneumoniae*, although the functionality of the staphylococcal proteins was reduced compared to the native $CozE^{Spn}$.

$CozE^{Spn}$ was identified as an essential regulator of cell elongation in *S. pneumoniae*, working through interactions with the $MreCD^{Spn}$ and $PBP1a^{Spn}$ [25]. The results presented here suggest that CozE proteins in bacteria have additional functionalities and may act at an earlier stage of cell division to mediate proper spatial and temporal control. During the bacterial cell cycle, DNA replication, chromosome segregation, cell division and cell wall synthesis need to be coordinated spatially and temporally. The uncontrolled cell division occurring in *S. aureus* cells lacking CozEa and CozEb, may thus further result in the pleiotropic effects we observed, such as aberrant chromosome replication/segregation, cell lysis and variable cell sizes. Future studies are required to unravel in more detail the molecular mode of action by which CozE proteins work. The CozE-mediated control of cell division seems to be a conserved feature between spherical *S. aureus* and ovococcal *S. pneumoniae*. Since genes encoding these proteins are widespread, it will be interesting to unravel how CozE proteins function in bacterial cells of various shapes.

Materials and methods

Bacterial strains, growth conditions and transformation

Bacterial strains used in this study are listed in S2 Table. *S. aureus* was routinely grown at 37°C in BHI broth with shaking or on brain-heart-infusion (BHI) agar plates at 37°C. When appropriate, 5 µg/ml erythromycin, 10 µg/ml chloramphenicol or 100 µg/ml spectinomycin was added for selection. For induction of gene expression, different concentrations of IPTG was added. *S. pneumoniae* was grown in C medium [43] at 37°C without shaking or on TH agar plates at 37°C. When appropriate, 400 µg/ml kanamycin, 200 µg/ml streptomycin or 100 µg/ml spectinomycin was added to the growth medium for selection. *Escherichia coli* was grown at 37°C in LB medium with shaking or on LA plates at 37°C with 100 µg/ml ampicillin or 50 µg/ml kanamycin added for selection.

Transformation of *E. coli* was performed with a standard heat shock protocol. *S. aureus* was transformed with electroporation using plasmid DNA isolated from *E. coli* DC10B [44] or IM08B [45]. Preparation of electrocompetent cells and electroporation were performed essentially as described before [46]. Constructs were introduced into *S. pneumoniae* using natural transformation as described before [22].

Construction of plasmids for the CRISPRi system

Construction of plasmid pLOW-dCas9. The *dcas9* gene was amplified from plasmid pJWV102-dcas9 [27] using primers mk41 and mk42. The fragment and the vector pLOW-ftsZ-m(sf)gfp were both digested with SalI and NotI and ligated to produce the pLOW-dCas9 construct where *dcas9* is placed downstream of an IPTG-inducible promoter. The ligation was transformed into *E. coli* IM08B with ampicillin selection and correct construct was verified by PCR and sequencing. All plasmids in this study are listed in S3 Table, while all primers are listed in S4 Table.

Constructions of plasmids expressing single guide RNA. The single guide RNA (sgRNA) construct, containing a transcriptionally isolated sgRNA (see Fig 2) driven by a constitutive promoter, was cut out from vector pPEPX-sgRNA(*luc*) [27] using PstI and BamHI. The fragment was ligated into the

corresponding sites of vector pCG248 [30] (thus removing the *xyl*/*tet* regulatory system from this vector) to produce pCG248-sgRNA(*luc*). The construct was verified by sequencing.

New sgRNAs were then made by replacing the 20 nt base-pairing region with an inverse PCR approach; using the pCG248-sgRNA(*luc*) as template, new sgRNA-plasmids were amplified using one reverse phosphorylated primer mk200 annealing immediately upstream of the sgRNA, combined with a gene-specific forward primer containing the base-pairing region as overlaps. The product was treated with DpnI to remove the template plasmid and ligated using T4 DNA ligase prior to transformation into *E. coli* IM08B with ampicillin selection. Constructs were verified by sequencing. The resulting plasmids were named pCG248-sgRNA(x), where x denotes the name of the gene to be targeted. Selection of the gene-specific base pairing region to be used was done using established criteria [27, 28].

For construction of the double-sgRNAs targeting both *cozEa* and *cozEb*, the fragment containing the sgRNA(*cozEb*) was cut out from the plasmid pCG248-sgRNA(*cozEb*) using restriction sites PstI and BamHI. The resulting fragment was ligated into the PstI and BglII sites of plasmid pCG248-sgRNA(*cozEa*). The resulting plasmid, pCG248-sgRNA(*cozEa-cozEb*), expresses two sgRNAs targeting both *cozEa* and *cozEb*. See also Fig S2.

CRISPR interference. In order to obtain *S. aureus* strains for CRISPRi, the plasmid pLOW-dCas9 was first introduced with erythromycin selection. Then, in a second step, the sgRNA-containing plasmid pCG248(x), was introduced with combined chloramphenicol and erythromycin selection (in order to retain both plasmids). Cells were then grown in the presence of IPTG to induce expression of *dcas9*.

S. aureus plasmid and strain construction

Construction of strain with constitutive GFP expression. A fragment containing a spectinomycin resistance gene and a gene encoding a monomeric superfolder GFP, *m(sf)gfp*, was first assembled by overlap extension PCR. The spectinomycin resistance cassette was amplified from pCN55 [47] using primers mk203 and mk204. The *m(sf)gfp* gene was amplified from plasmid pMK17 [48] using primer im84 and im2. The primers mk204 and im84 contain overlapping sequence, and the *spc-m(sf)gfp*

fragment could then be assembled in a second amplification step with outer primers mk203 and im2. The resulting fragment contains EcoRI sites on both ends introduced by overhangs in the primers. The fragment was digested with EcoRI and ligated into the corresponding site of plasmid pMAD-int2-luc. The ligation was transformed in *E. coli* IM08B with ampicillin selection. The resulting construct, pMAD-int2-luc-spc-gfp, was verified by PCR and sequencing. The temperature sensitive pMAD-derivative vector [26] was transformed in *S. aureus* RN4220 at 30°C with erythromycin and X-gal selection. Integration of the plasmid into the chromosome and excision to construct the integration of P3-luc-spc-gfp in the *int*-locus [49] was performed as described [26] with spectinomycin selection.

Construction of Δ*cozEa::spc* and Δ*cozEb*::*spc*. Vectors for deletion of *cozEa* and *cozEb* were made in pMAD. The constructions *cozEa::spc* and *cozEb::spc* were first assembled by overlap extension PCR as follows: The spectinomycin resistance cassette (*spc*) was amplified from plasmid pCN55 using primers mk188 and mk189. The *cozEa* upstream region was amplified with primers mk182 and mk184 and the downstream fragment with primers mk185 and mk187. The three fragments were assembled using overlap extension PCR and amplified using the outer primers mk183 and mk186. The outer primers contain restriction sites for NcoI and BamHI, and the cozEa_up – spc – cozEa_down fragment was ligated into the NcoI and BamHI sites of pMAD. The ligation was transformed into *E. coli* IM08B and correct transformants containing the pMAD-*cozEa*::*spc* plasmid were verified by PCR and sequencing.

pMAD-*cozEb*::*spc* plasmid was constructed in a similar way. The *spc* fragment was amplified in the same manner as above. The *cozEb* up- and downstream regions were amplified using primers mk190 and mk192, and mk193 and mk195, respectively. The resulting fragments were fused by overlap extension PCR using primers mk191 and mk194, and the resulting fragment (cozEb_up – spc – cozEb_down), was ligated into the NcoI and BamHI sites of pMAD.

Finally, the pMAD-*cozEa*::*cam* plasmid was constructed by amplifying the upstream region with primers mk183 and mk259 and the downstream region with primers mk260 and mk186. A chloramphenicol resistance cassette was amplified from plasmid pRAB11 [30], using primers mk257

and mk258. The fragments were fused by overlap extension PCR and ligated into the NcoI and BamHI sites of pMAD.

Construction of the deletion strain was done as previously described for the temperature sensitive pMAD system. Briefly, the plasmids were transformed into *S. aureus* SH1000 with erythromycin selection with incubation at permissive temperature of 30°C. X-gal was also added to the transformation plates and blue colonies were re-streaked once at 30°C. One colony was then picked and grown in medium without selection at 30°C for 2 hours before the tube was transferred to non-permissive temperature for plasmid replication (43°C) for 6 hours. The culture was then plated on TSA with spectinomycin and X-gal at 43°C. White colonies, where double crossover had taken place to replace the gene of interest with the spectinomycin cassette were re-streaked on two separate plates to verify that they were spectinomycin resistant and erythromycin sensitive. Correct constructs were further verified by PCR and sequencing. The Δ*cozEa*::*spc* deletion strain was named SAMK24 and the Δ*cozEb*::*spc* deletion strain SAMK21.

Strain construction for *S. pneumoniae*

Construction of P_{comX}-*cozE*^{Spn}, P_{comX}-*cozEa*, P_{comX}-*cozEb* and deletion of *cozE*^{Spn}. The ectopic P_{comX}-*cozE*^{Spn} construct integrated in the *cpsO-cpnN* locus of *S. pneumoniae* has been described previously [21].

For construction of P_{comX}-*cozEa* and P_{comX}-*cozEb*, primers gs693/gs694 were used to amplify the *cozEa* gene and primers GS691/GS692 were used to amplify the *cozEb* gene, both using genomic DNA from *S. aureus* SH1000 as template. Using strain *S. pneumoniae* SPH131 as template, the P_{comX} and 800 bp upstream region in the *cpsO-cpsN* locus were amplified with primers khb31/khb33 and the *cpsO-cpsN* downstream fragment was amplified with primers khb34/khb36. The three fragments contain overlapping sequences introduced in the primers, and they were assembled by overlap extension PCR to create P_{comX}-*cozEa* and P_{comX}-*cozEb*. The constructs were transformed into strain SPH131 (containing a Janus cassette in the *cpsO-cpsN* locus) and transformants were selected on plates with streptomycin. The resulting strains were named GS1169 and GS1170.

The native pneumococcal *cozE*^{Spn} (*spr0777*) gene was replaced with a Janus cassette in strains GS1169, GS1170 and KHB432 as described before [21]. Since *spr0777* is essential, different concentrations of the transcription inducer ComS (0, 0.2 and 2 µM) were added during all transformation steps to induce expression of the various *cozE* genes from the P_{comX} promoter. Transformants were selected on plates containing kanamycin. The number of colonies were counted and the transformants were screened for the presence of the pneumococcal *cozE*^{Spn} gene with primers gs337 and gs338 for each ComS concentration.

Construction of *ezrA*^{Spn}*-yfp*. An *ezrA-yfp_spc* fragment was assembled by overlap extension PCR. The ezrA_up fragment was amplified from *S. pneumoniae* R6 using primers mk288 and mk289, while the ezrA_down fragment was amplified using primers mk292 and mk293. The *yfp_spc* fragment was amplified from strain MK123 using primers mk290 and mk291. Due to overhangs in the primers, the three fragments could be assembled using outer primers mk301 and mk302, to produce the *ezrA-yfp_spc* fragment, which integrates in the pneumococcal chromosome to replace the native *ezrA* gene with an *ezrA-yfp* fusion gene. The fragment was transformed into *S. pneumoniae* and transformants were selected on plates with spectinomycin. Correct transformants were verified by PCR.

Bacterial two-hybrid analysis

Construction of plasmids. Genes of interest were fused in frame to either 5` end or 3` end of either the T18 or the T25 domain of adenylate cyclase from *Bordetella pertussis* using the four vectors (pKT25, pKNT25, pUT18, pUT18C) provided by the manufacturer (Euromedex). Primers used for amplification of the genes are listed in S4 Table. The amplified fragments were digested (restriction sites indicated in the S4 Table) and ligated into the corresponding restriction sites in the vectors. Ligations were transformed into *E. coli* XL1-Blue cells, and selected on 1% glucose LA plates containing either 50 µg/ml kanamycin or 100 µg/ml ampicillin. Correct plasmids were verified by PCR and sequencing

Bacterial two-hybrid assay. Bacterial two-hybrid assays [33] were performed as described by the manufacturer (Euromedex). Briefly, two plasmids, one containing a fusion to the T18 domain and the other a fusion to the T25 domain, were co-transformed into *E. coli* BTH101. The transformants were selected on LA plates containing 50 µg/ml kanamycin and 100 µg/ml ampicillin for selection. Five random colonies were picked per assay and grown in liquid LB containing kanamycin and ampicillin to OD_{600} 0.3, before 2.5 µl of the cell culture was spotted on LA plates supplemented with 50 µg/ml kanamycin, 100 µg/ml ampicillin, 40 µg/ml of X-gal and 0.5 mM IPTG. The plates were incubated protected from light at 30°C for 20 h to 48 h. Positive interactions are indicated by appearance of blue colonies, while white colonies indicate no interaction.

Isolation of peptidoglycan and HPLC-analysis

Strains GS1167 and SAMK15 were inoculated in 60 ml BHI containing 10 µg/ml chloramphenicol and 5 µg/ml erythromycin. At OD_{600} 0.2 these cells were transferred to 1.5 liters of BHI containing 10 µg/ml chloramphenicol, 5 µg/ml erythromycin and 150 µM IPTG. When reaching OD_{600} = 0.3, cells were harvested at 8000 x *g* for 10 minutes. Peptidoglycan was isolated according to the protocol described by Vollmer [50]. The isolated peptidoglycan was lyophilized and resuspended in water to a final concentration of 50 mg/ml.

HPLC analysis of muropeptides was performed as described by Vollmer [50] and Carvalho *et al* [51] with minor changes. Briefly, to remove cell wall teichoic acids, ten milligrams of purified peptidoglycan were treated with 1.5 ml 48% HF at 4°C for 48 hours with gentle mixing. The HF-treated peptidoglycan was collected by centrifugation at 20 000 x *g* for 30 minutes and washed two times with 1.5 ml of dH_2O, once with 1.5 ml of 50 mM Tris-HCl (pH 7.4) and finally twice with 1.5 ml of dH_2O. One mg of HF-treated peptidoglycan was digested with 5000 U mutanolysin at 37 °C for 18-20 hours in a final volume of 100 µl containing 12.5 mM NaH_2PO_4 (pH 5.5). The sample was boiled for 20 minutes before insoluble material was removed by centrifugation at 20 000 *x g* for 30 minutes. The supernatant was added with 0.5 M Na-borate pH 9.0 (1:1 volume) and treated with 1-2 mg of Na-borohydride for 30 minutes at room temperature to reduce the sugars. The reaction was stopped by

adjusting the pH to 2.0 using 20 % phosphoric acid. Muropeptides were separated on a C18 column (Vydac 218TP C18 5 mm, Grace Davison Discovery Sciences) at 52 °C using a linear 155-minutes gradient of methanol from 5-30% in 0.1 M NaH_2PO_4 (pH 2.0) at a flow rate of 0.5 ml/min. Eluted muropeptides were detected at 206 nm.

Phase contrast and fluorescence microscopy

Microscopy was performed on a Zeiss AxioObserver with ZEN Blue software. Images were captured with an ORCA-Flash4.0 V2 Digital CMOS camera (Hamamatsu Photonics) through a 100x PC objective. For fluorescence microscopy, HPX 120 Illuminator (Zeiss) was used as a light source. Image analysis was performed using MicrobeJ [52] and plotting was done in RStudio.

Transmission electron microscopy

Strains SH1000, SAMK21 and SAMK24 were grown to OD_{600} = 0.4 prior to sample preparation. GS1167 and SAMK15 were pre-grown to OD_{600} = 0.1, after which the cultures were diluted 64-fold in medium with or without 150 µg/ml IPTG and grown until OD_{600} = 0.3. Cells were fixed by adding a solution of 4 % parafomaldehyd (w/v) and 5 % glutardialdehyd (w/v) in 1 x PBS pH 7.4 to the cell culture in a 1:1 ratio. The fixation mix was incubated 1 hour in room temperature and kept overnight at 4 °C. The next day the cells were washed three times in PBS and three times in cacodylate buffer (CaCo) before being post-fixed for one hour in 1 % OsO_4 in 0.1 M CaCo. Cells were washed three times in CaCo buffer, infiltrated in 3 % agarose and washed again three times in CaCo buffer. The samples were then dehydrated in a gradient series of 70 %, 90 %, 96 %, and 100 % ethanol (15 min for each ethanol concentration). Infiltration in LR White resin was then performed in multiple steps; LR White resin:EtOH in a ratio 1:3 was first incubated overnight, then a ratio of 1:1 for 7 hours, a ratio of 3:1 overnight and finally 100 % LR White resin overnight. Then the samples were embedded in 100 % LR White resin at 60 °C for 72 hours. Thin sections were made and stained with uranyl acetate and potassium permanganate. The samples were analyzed in a FEI MORGAGNI 268 electron microscope.

Growth assays

Growth assays were performed in a Synergy H1 Hybrid Reader (BioTek) microtiter plate reader at 37°C. Five ml of cell culture were grown to exponential phase, OD_{600} = 0.4 before being harvested, resuspended in fresh BHI medium and diluted to OD_{600} = 0.05. Appropriate antibiotics were always present. Each well in the microtiter plate was added 280 µl diluted cell culture. IPTG (150 µM) was added to the wells when appropriate. Measurements of OD_{600} were taken every 10th minute throughout growth.

Genome resequencing and analysis

Genomic DNA was isolated from *S. aureus* SH1000, SAMK21 and SAMK24 using the NucleoBond AXG 100 kit (Macherey-Nagel). For *S. aureus* SH1000, library for sequencing was created using the Nextera XT DNA library preparation kit (Illumina), and the sequencing was performed using an in-house Illumina MiSeq. For SAM21 and SAMK24, PCR-free library preparation and sequencing (HiSeq4000 PE151) was performed by BGI Hong Kong. Sequences assembly to the *S. aureus* NCTC8325 reference genome and SNP detection were done using Geneious version 10.1 [53].

Acknowledgements

We would like to thank Lene C. Hermansen at the Imaging Center, NMBU, for help with transmission electron microscopy and Davide Porcellato, NMBU, for help with genome sequencing.

References

1. Pinho MG, Kjos M, Veening JW. How to get (a)round: mechanisms controlling growth and division of coccoid bacteria. Nat Rev Microbiol. 2013;11(9):601-14. doi: 10.1038/nrmicro3088.

2. Grice EA, Segre JA. The skin microbiome. Nat Rev Microbiol. 2011;9(4):244-53. doi: 10.1038/nrmicro2537.

3. Rasigade JP, Vandenesch F. *Staphylococcus aureus*: a pathogen with still unresolved issues. Infect Genet Evol. 2014;21:510-4. doi: 10.1016/j.meegid.2013.08.018.

4. Foster TJ, Geoghegan JA, Ganesh VK, Hook M. Adhesion, invasion and evasion: the many functions of the surface proteins of *Staphylococcus aureus*. Nat Rev Microbiol. 2014;12(1):49-62. doi: 10.1038/nrmicro3161.

5. Monteiro JM, Fernandes PB, Vaz F, Pereira AR, Tavares AC, Ferreira MT, et al. Cell shape dynamics during the staphylococcal cell cycle. Nat Commun. 2015;6:8055. doi: 10.1038/ncomms9055.

6. Zhou X, Halladin DK, Rojas ER, Koslover EF, Lee TK, Huang KC, et al. Bacterial division. Mechanical crack propagation drives millisecond daughter cell separation in *Staphylococcus aureus*. Science. 2015;348(6234):574-8. doi: 10.1126/science.aaa1511.

7. Pinho MG, Errington J. Dispersed mode of *Staphylococcus aureus* cell wall synthesis in the absence of the division machinery. Mol Microbiol. 2003;50(3):871-81.

8. Pinho MG, Errington J. A *divIVA* null mutant of *Staphylococcus aureus* undergoes normal cell division. FEMS Microbiol Lett. 2004;240(2):145-9. doi: 10.1016/j.femsle.2004.09.038.

9. Steele VR, Bottomley AL, Garcia-Lara J, Kasturiarachchi J, Foster SJ. Multiple essential roles for EzrA in cell division of *Staphylococcus aureus*. Mol Microbiol. 2011;80(2):542-55. doi: 10.1111/j.1365-2958.2011.07591.x.

10. Bottomley AL, Kabli AF, Hurd AF, Turner RD, Garcia-Lara J, Foster SJ. *Staphylococcus aureus* DivIB is a peptidoglycan-binding protein that is required for a morphological checkpoint in cell division. Mol Microbiol. 2014. doi: 10.1111/mmi.12813.

11. Jorge AM, Hoiczyk E, Gomes JP, Pinho MG. EzrA contributes to the regulation of cell size in *Staphylococcus aureus*. PLoS One. 2011;6(11):e27542. doi: 10.1371/journal.pone.0027542.

12. Pang T, Wang X, Lim HC, Bernhardt TG, Rudner DZ. The nucleoid occlusion factor Noc controls DNA replication initiation in *Staphylococcus aureus*. PLoS Genet. 2017;13(7):e1006908. doi: 10.1371/journal.pgen.1006908.

13. Veiga H, Jorge AM, Pinho MG. Absence of nucleoid occlusion effector Noc impairs formation of orthogonal FtsZ rings during *Staphylococcus aureus* cell division. Mol Microbiol. 2011;80(5):1366-80. doi: 10.1111/j.1365-2958.2011.07651.x.

14. Bottomley AL, Liew ATF, Kusuma KD, Peterson E, Seidel L, Foster SJ, et al. Coordination of chromosome segregation and cell division in *Staphylococcus aureus*. Front Microbiol. 2017;8:1575. doi: 10.3389/fmicb.2017.01575.

15. Ducret A, Grangeasse C. Bacterial physiology: Wrapping the cell in a CozE shell. Nat Microbiol. 2017;2:16262. doi: 10.1038/nmicrobiol.2016.262.

16. van Raaphorst R, Kjos M, Veening JW. Chromosome segregation drives division site selection in *Streptococcus pneumoniae*. Proc Natl Acad Sci U S A. 2017;114(29):E5959-E68. doi: 10.1073/pnas.1620608114.

17. Fleurie A, Lesterlin C, Manuse S, Zhao C, Cluzel C, Lavergne JP, et al. MapZ marks the division sites and positions FtsZ rings in *Streptococcus pneumoniae*. Nature. 2014;516(7530):259-62. doi: 10.1038/nature13966.

18. Holeckova N, Doubravova L, Massidda O, Molle V, Buriankova K, Benada O, et al. LocZ is a new cell division protein involved in proper septum placement in *Streptococcus pneumoniae*. MBio. 2014;6(1):e01700-14. doi: 10.1128/mBio.01700-14.

19. Fleurie A, Manuse S, Zhao C, Campo N, Cluzel C, Lavergne JP, et al. Interplay of the serine/threonine-kinase StkP and the paralogs DivIVA and GpsB in pneumococcal cell elongation and division. PLoS Genet. 2014;10(4):e1004275. doi: 10.1371/journal.pgen.1004275.

20. Rued BE, Zheng JJ, Mura A, Tsui HT, Boersma MJ, Mazny JL, et al. Suppression and synthetic-lethal genetic relationships of DgpsB mutations indicate that GpsB mediates protein phosphorylation and penicillin-binding protein interactions in *Streptococcus pneumoniae* D39. Mol Microbiol. 2017;103(6):931-57. doi: 10.1111/mmi.13613.

21. Straume D, Stamsas GA, Berg KH, Salehian Z, Havarstein LS. Identification of pneumococcal proteins that are functionally linked to penicillin-binding protein 2b (PBP2b). Mol Microbiol. 2017;103(1):99-116. doi: 10.1111/mmi.13543.

22. Stamsas GA, Straume D, Ruud Winther A, Kjos M, Frantzen CA, Havarstein LS. Identification of EloR (Spr1851) as a regulator of cell elongation in *Streptococcus pneumoniae*. Mol Microbiol. 2017. doi: 10.1111/mmi.13748.

23. Beilharz K, Novakova L, Fadda D, Branny P, Massidda O, Veening JW. Control of cell division in *Streptococcus pneumoniae* by the conserved Ser/Thr protein kinase StkP. Proc Natl Acad Sci U S A. 2012;109(15):E905-13. doi: 10.1073/pnas.1119172109.

24. Zheng JJ, Perez AJ, Tsui HT, Massidda O, Winkler ME. Absence of the KhpA and KhpB (JAG/EloR) RNA-binding proteins suppresses the requirement for PBP2b by overproduction of FtsA in *Streptococcus pneumoniae* D39. Mol Microbiol. 2017. doi: 10.1111/mmi.13847.

25. Fenton AK, Mortaji LE, Lau DT, Rudner DZ, Bernhardt TG. CozE is a member of the MreCD complex that directs cell elongation in *Streptococcus pneumoniae*. Nat Microbiol. 2016;2:16237. doi: 10.1038/nmicrobiol.2016.237.

26. Arnaud M, Chastanet A, Debarbouille M. New vector for efficient allelic replacement in naturally nontransformable, low-GC-content, gram-positive bacteria. Appl Environ Microbiol. 2004;70(11):6887-91. doi: 10.1128/AEM.70.11.6887-6891.2004.

27. Liu X, Gallay C, Kjos M, Domenech A, Slager J, van Kessel SP, et al. High-throughput CRISPRi phenotyping identifies new essential genes in *Streptococcus pneumoniae*. Mol Syst Biol. 2017;13(5):931. doi: 10.15252/msb.20167449.

28. Peters JM, Colavin A, Shi H, Czarny TL, Larson MH, Wong S, et al. A comprehensive, CRISPR-based functional analysis of essential genes in bacteria. Cell. 2016;165(6):1493-506. doi: 10.1016/j.cell.2016.05.003.

29. Liew AT, Theis T, Jensen SO, Garcia-Lara J, Foster SJ, Firth N, et al. A simple plasmid-based system that allows rapid generation of tightly controlled gene expression in *Staphylococcus aureus*. Microbiology. 2011;157(Pt 3):666-76. doi: 10.1099/mic.0.045146-0.

30. Helle L, Kull M, Mayer S, Marincola G, Zelder ME, Goerke C, et al. Vectors for improved Tet repressor-dependent gradual gene induction or silencing in *Staphylococcus aureus*. Microbiology. 2011;157(Pt 12):3314-23. doi: 10.1099/mic.0.052548-0.

31. Pereira SF, Henriques AO, Pinho MG, de Lencastre H, Tomasz A. Role of PBP1 in cell division of *Staphylococcus aureus*. J Bacteriol. 2007;189(9):3525-31. doi: 10.1128/jb.00044-07.

32. Pereira SF, Henriques AO, Pinho MG, de Lencastre H, Tomasz A. Evidence for a dual role of PBP1 in the cell division and cell separation of *Staphylococcus aureus*. Mol Microbiol. 2009;72(4):895-904. doi: 10.1111/j.1365-2958.2009.06687.x.

33. Karimova G, Dautin N, Ladant D. Interaction network among *Escherichia coli* membrane proteins involved in cell division as revealed by bacterial two-hybrid analysis. J Bacteriol. 2005;187(7):2233-43. doi: 10.1128/jb.187.7.2233-2243.2005.

34. Berg KH, Biornstad TJ, Straume D, Havarstein LS. Peptide-regulated gene depletion system developed for use in *Streptococcus pneumoniae*. J Bacteriol. 2011;193(19):5207-15. doi: 10.1128/JB.05170-11.

35. Sung CK, Li H, Claverys JP, Morrison DA. An *rpsL* cassette, janus, for gene replacement through negative selection in *Streptococcus pneumoniae*. Appl Environ Microbiol. 2001;67(11):5190-6. doi: 10.1128/aem.67.11.5190-5196.2001.

36. Dong X, Jin Y, Ming D, Li B, Dong H, Wang L, et al. CRISPR/dCas9-mediated inhibition of gene expression in *Staphylococcus aureus*. J Microbiol Methods. 2017;139:79-86. doi: 10.1016/j.mimet.2017.05.008.

37. Zhao C, Shu X, Sun B. Construction of a gene knockdown system based on catalytically inactive ("dead") Cas9 (dCas9) in *Staphylococcus aureus*. Appl Environ Microbiol. 2017;83(12). doi: 10.1128/AEM.00291-17.

38. Anderson JC, Dueber JE, Leguia M, Wu GC, Goler JA, Arkin AP, et al. BglBricks: A flexible standard for biological part assembly. J Biol Eng. 2010;4(1):1. doi: 10.1186/1754-1611-4-1.

39. Pereira AR, Hsin J, Krol E, Tavares AC, Flores P, Hoiczyk E, et al. FtsZ-dependent elongation of a coccoid bacterium. MBio. 2016;7(5). doi: 10.1128/mBio.00908-16.

40. Tavares AC, Fernandes PB, Carballido-Lopez R, Pinho MG. MreC and MreD proteins are not required for growth of *Staphylococcus aureus*. PLoS One. 2015;10(10):e0140523. doi: 10.1371/journal.pone.0140523.

41. Levin PA, Kurtser IG, Grossman AD. Identification and characterization of a negative regulator of FtsZ ring formation in *Bacillus subtilis*. Proc Natl Acad Sci U S A. 1999;96(17):9642-7.

42. Claessen D, Emmins R, Hamoen LW, Daniel RA, Errington J, Edwards DH. Control of the cell elongation-division cycle by shuttling of PBP1 protein in *Bacillus subtilis*. Mol Microbiol. 2008;68(4):1029-46. doi: 10.1111/j.1365-2958.2008.06210.x.

43. Lacks S, Hotchkiss RD. A study of the genetic material determining an enzyme in Pneumococcus. Biochim Biophys Acta. 1960;39:508-18.

44. Monk IR, Shah IM, Xu M, Tan MW, Foster TJ. Transforming the untransformable: application of direct transformation to manipulate genetically *Staphylococcus aureus* and *Staphylococcus epidermidis*. MBio. 2012;3(2). doi: 10.1128/mBio.00277-11.

45. Monk IR, Tree JJ, Howden BP, Stinear TP, Foster TJ. Complete bypass of restriction systems for major *Staphylococcus aureus* lineages. MBio. 2015;6(3):e00308-15. doi: 10.1128/mBio.00308-15.

46. Lofblom J, Kronqvist N, Uhlen M, Stahl S, Wernerus H. Optimization of electroporation-mediated transformation: *Staphylococcus carnosus* as model organism. J Appl Microbiol. 2007;102(3):736-47. doi: 10.1111/j.1365-2672.2006.03127.x.

47. Charpentier E, Anton AI, Barry P, Alfonso B, Fang Y, Novick RP. Novel cassette-based shuttle vector system for gram-positive bacteria. Appl Environ Microbiol. 2004;70(10):6076-85. doi: 10.1128/aem.70.10.6076-6085.2004.

48. Kjos M, Miller E, Slager J, Lake FB, Gericke O, Roberts IS, et al. Expression of *Streptococcus pneumoniae* bacteriocins is induced by antibiotics via regulatory interplay with the competence system. PLoS Pathog. 2016;12(2):e1005422. doi: 10.1371/journal.ppat.1005422.

49. Fagerlund A, Granum PE, Havarstein LS. *Staphylococcus aureus* competence genes: mapping of the SigH, ComK1 and ComK2 regulons by transcriptome sequencing. Mol Microbiol. 2014;94(3):557-79. doi: 10.1111/mmi.12767.

50. Vollmer W. Preparation and analysis of pneumococcal murein (peptidoglycan). In: Hakenbeck R, Chhatwal S, editors. Molecular Biology of Streptococci. Norfolk, UK.: Horizon Bioscience; 2007. p. 531-6.

51. Carvalho F, Atilano ML, Pombinho R, Covas G, Gallo RL, Filipe SR, et al. L-rhamnosylation of *Listeria monocytogenes* wall teichoic acids promotes resistance to antimicrobial peptides by delaying

interaction with the membrane. PLoS Pathog. 2015;11(5):e1004919. doi: 10.1371/journal.ppat.1004919.

52. Ducret A, Quardokus EM, Brun YV. MicrobeJ, a tool for high throughput bacterial cell detection and quantitative analysis. Nat Microbiol. 2016;1(7):16077. doi: 10.1038/nmicrobiol.2016.77.

53. Kearse M, Moir R, Wilson A, Stones-Havas S, Cheung M, Sturrock S, et al. Geneious Basic: an integrated and extendable desktop software platform for the organization and analysis of sequence data. Bioinformatics. 2012;28(12):1647-9. doi: 10.1093/bioinformatics/bts199.

Figure captions

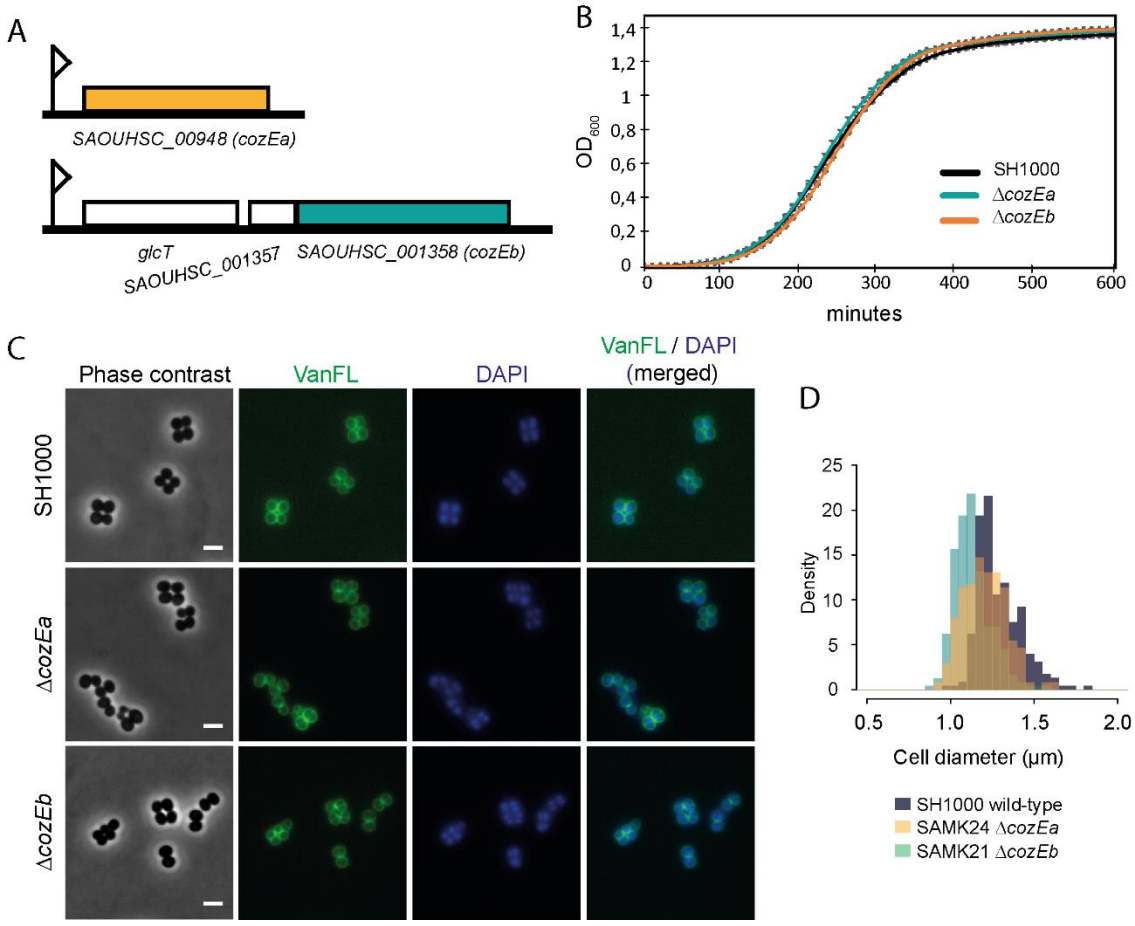

Fig 1. *cozEa* and *cozEb* of *S. aureus*. (**A**) Genetic organization of the *cozEa* (SAOUHSC_00948) and *cozEb* (SAOUHSC_01358) genetic loci. (**B**) Growth curves SH1000 wild-type, SAMK24 (Δ*cozEa*) and SAMK21 (Δ*cozEb*) in BHI medium at 37°C (**C**) Micrographs of SH1000, SAMK21 and SAMK24. Phase contrast (PC) images and staining with fluorescent vancomycin (VanFL) and DAPI are shown as well as an overlay of the two latter. The scale bars are 2 µm. (**D**) Histogram of the cell diameters of SH1000, SAMK24 and SAMK21 (>250 cells analyzed per sample) as measured using MicrobeJ [52].

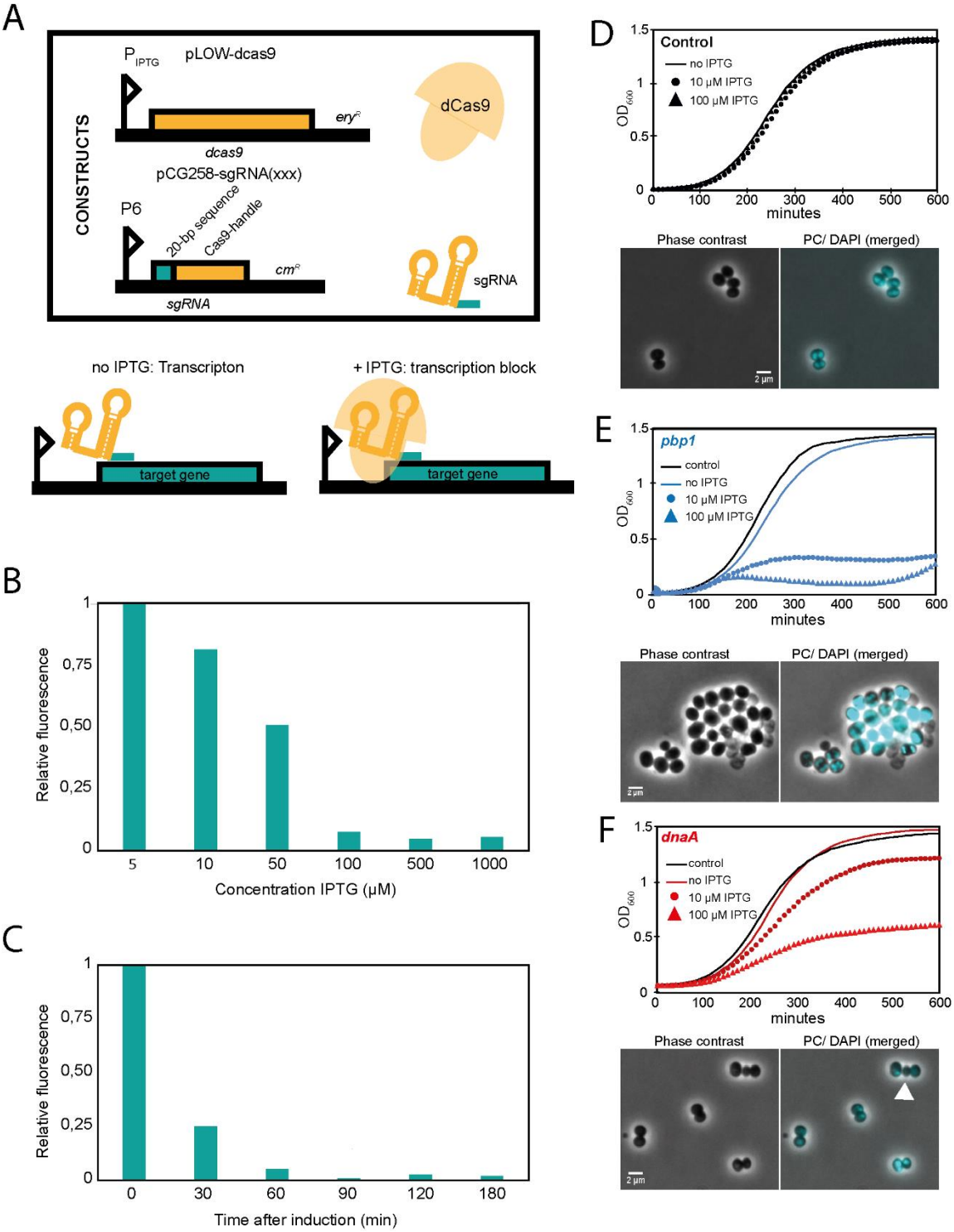

Fig 2. Two-plasmid CRISPR interference system for *S. aureus*. (**A**) Schematic representation of the plasmids carrying dCas9 and sgRNA. The sgRNA is constitutively expressed, while the level of dCas9 is controlled by the inducible P_{lac} promoter. Upon addition of IPTG, dCas9 will be expressed and the dCas9-sgRNA-DNA complex formation will lead to transcription block and knockdown of the target gene. (**B-C**) Knockdown of GFP expression in a strain constitutively expressing *m(sf)gfp* (SAMK56).

(**B**) Fluorescence after induction with various IPTG concentrations. The fluorescence values are given relative to the fluorescence of a non-depleted strain. The experiment was repeated twice with similar results. (**C**) The temporal dynamics of GFP depletion after addition of 100 µM IPTG. The fluorescence at the time of IPTG addition was set to 1, and measured at different time points. The experiment was repeated twice with similar results. (**D-F**) Growth and phenotypic characterization of cells with depletion of *pbp1* (**E**) and *dnaA* (**F**) Cells carrying sgRNA targeting *m(sf)gfp* are included as controls (**D**). Growth curves in BHI medium at 37°C and micrographs are shown. The arrowhead points to an example of an anucleate cell. The scale bars are 2 µm.

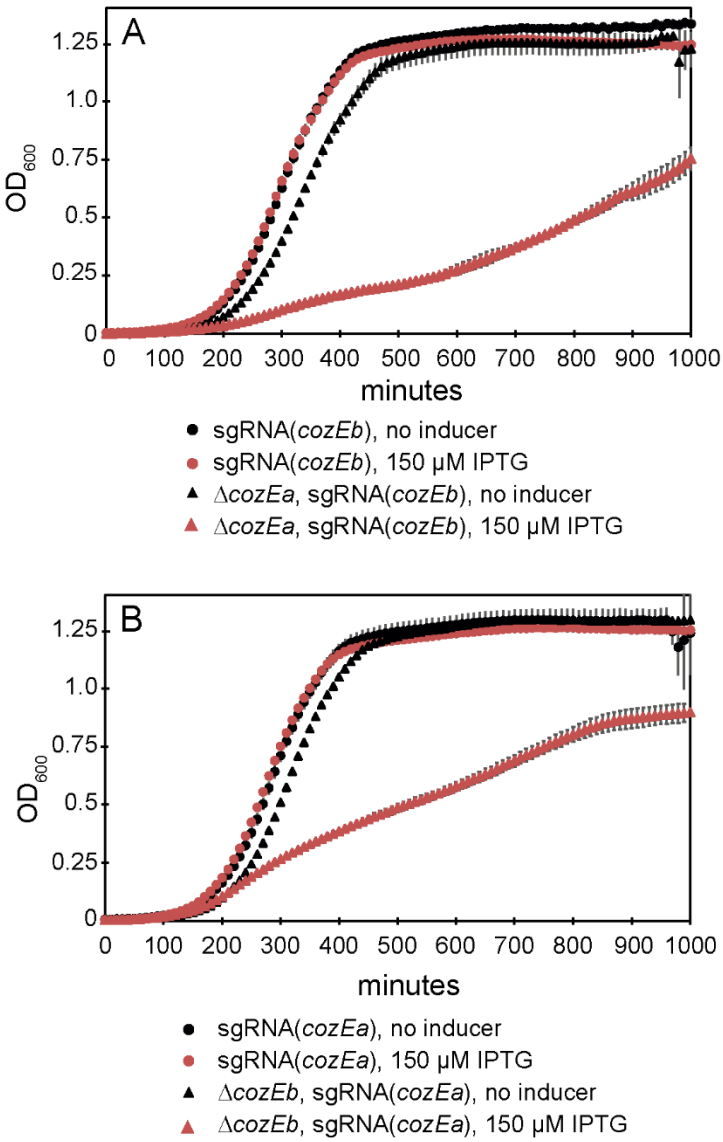

Fig 3. Functional redundancy of *cozEa* and *cozEb*. (**A**) Strains carrying sgRNA targeting *cozEb* in wild-type background (circles) compared to the Δ*cozEa* Δbackground (triangles). Growth curves with (red) or without (black) induction of dCas9 expression with 150 μM IPTG are shown. (**B**) Strains carrying sgRNA targeting *cozEa* in wild-type background (circles) compared to the Δ*cozEb* strain (triangles). Growth curves with (red) or without (black) induction of dCas9 expression with 150 μM IPTG are shown.

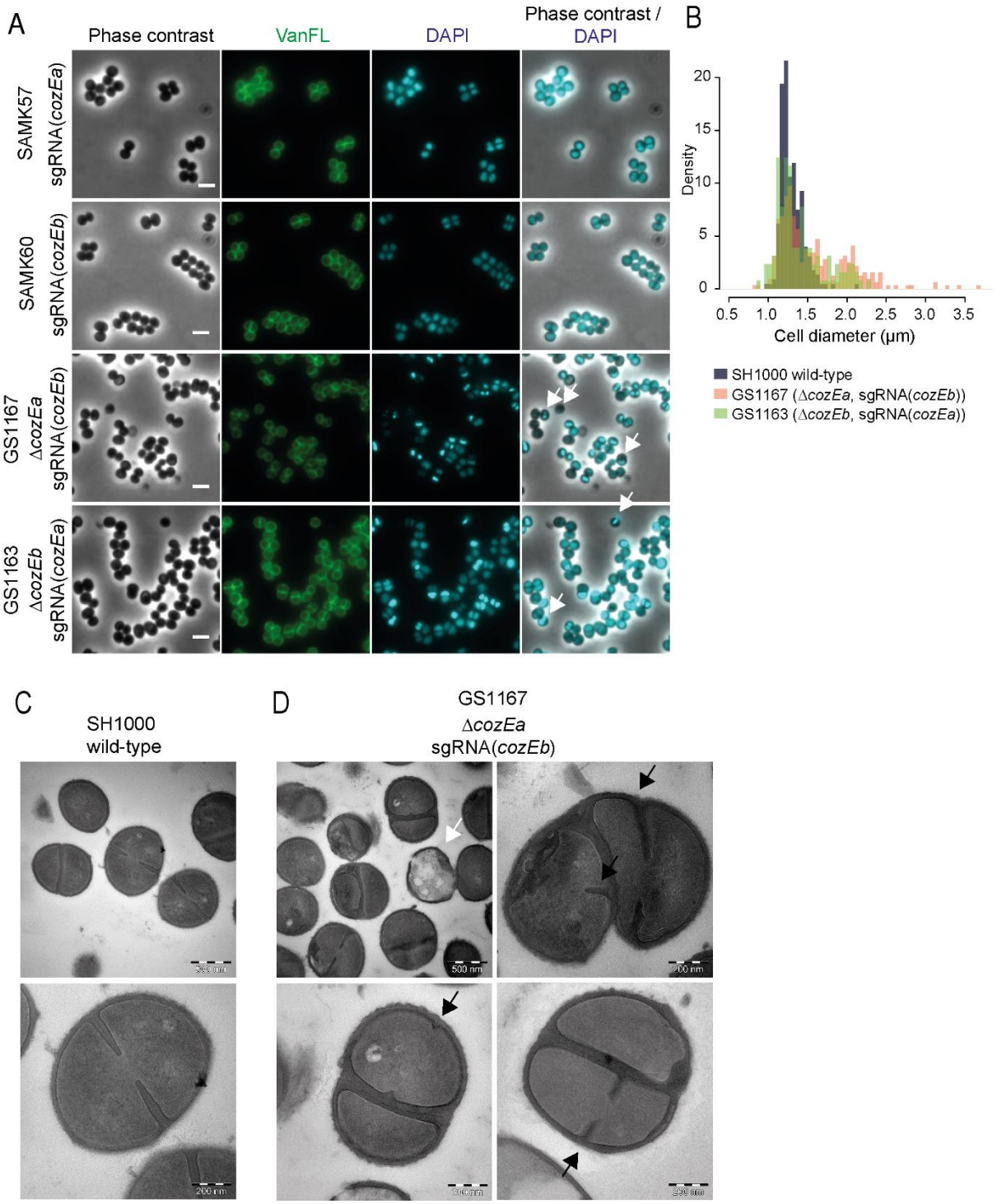

Fig 4. CozEa/CozEb phenotypes in *S. aureus* SH1000. (**A**) Phase contrast micrographs are shown to the left. The cells were also stained with fluorescent vancomycin and DAPI to visualize cell wall and the nucleoid, respectively. Overlay of DAPI and phase contrast images are shown. White arrows point to cell with aberrant nucleoids. The scale bars are 2 µm. (**B**) Histogram of cell diameter distribution for wild-type cells (grey) and Δ*cozEa*::*spc* with depleted *cozEb* (GS1167, orange) cells and Δ*cozEb*::*spc*

with depleted *cozEa* (GS1163, green) induced with 150 µM IPTG. (**C-D**) Transmission electron micrographs of wild-type cells (**C**, SH1000) and Δ*cozEa*::*spc* with depleted *cozEb* (D, GS1167) cells. The white arrow points to a lysed cell. Black arrows point to uncoordinated septum initiation in GS1167 cells. Two different magnifications are shown, as indicated by the scale bars.

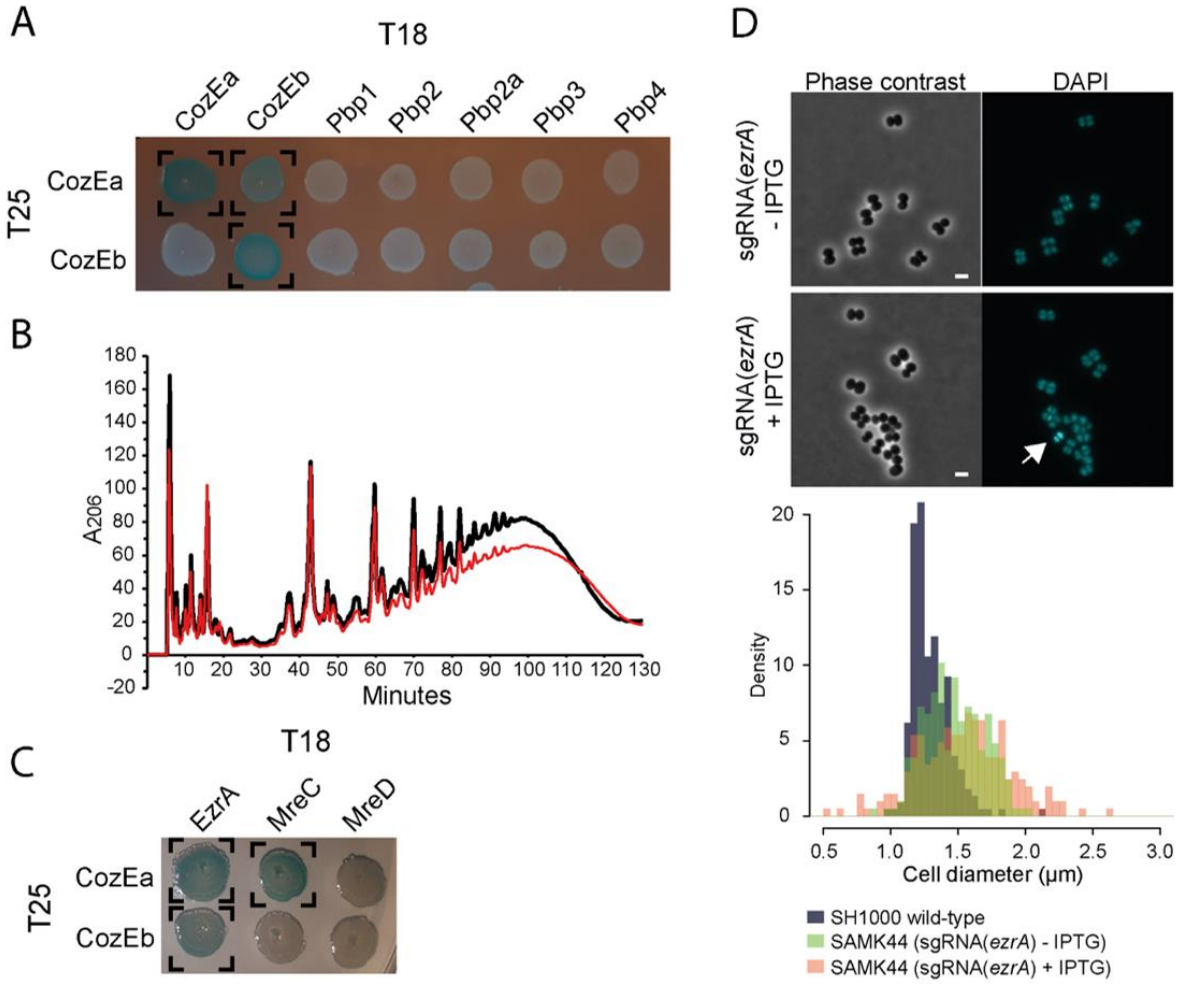

Fig 5. CozEa and CozEb interact with EzrA, but do not alter cell wall synthesis. (**A**) Bacterial two-hybrid analyses of interactions between CozEa and CozEb fused to the T25 domain with proteins fused to the T18. Positive interactions are observed as blue colonies and marked with brackets. (**B**) Cell wall muropeptide composition of SAMK15 control cells (black) and GS1167 depletion cells (red) induced with 150 mM IPTG for 4 hours as analyzed with UHPLC. (**C**) Bacterial two-hybrid analyses of interactions between CozEa and CozEb fused to the T25 domain with EzrA, MreC and MreD fused to the T18 domain. Positive interactions are observed as blue colonies and marked with brackets. (**D**) Phenotype of *ezrA* knockdown. Phase contrast micrographs and DAPI signal are shown for SAMK44 (CRISPRi targeting *ezrA*) with or without induction with 300 µM IPTG. The arrows point to cells with aberrant nucleoid staining. The scale bars are 2 µm. The lower panel shows cell diameter histograms of wild-type SH1000 cells as well as induced and non-induced SAMK44 cells.

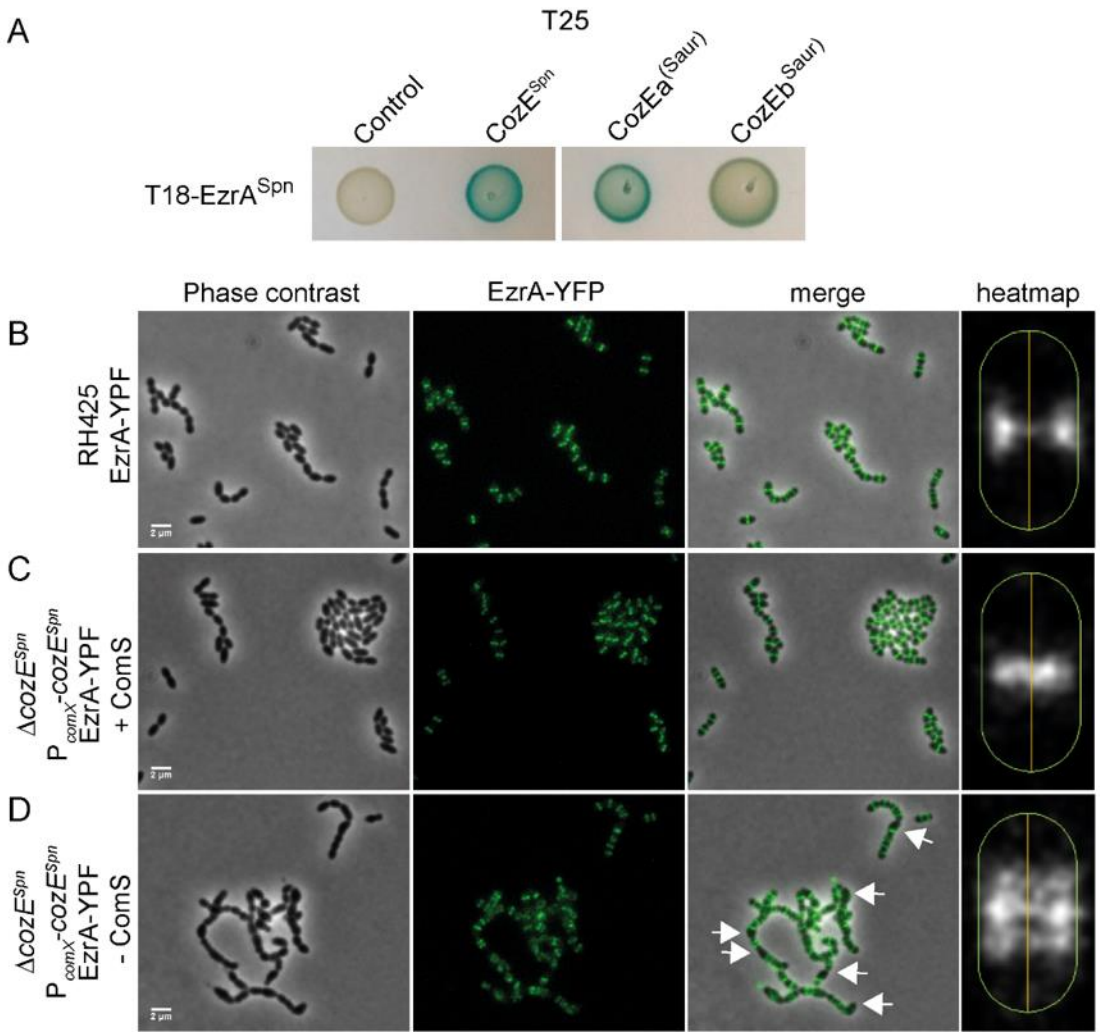

Fig 6. CozE^{Spn} controls division ring formation in *S. pneumoniae*. (**A**) Bacterial two-hybrid assay showing interactions between EzrA^{Spn} and different CozE-proteins. (**B-D**) Localization of EzrA-YFP in *S. pneumoniae*. Phase contrast and fluorescence are shown individually and merged. The localization of EzrA-YFP in the cells are also shown as heatmaps, as generated using MicrobeJ. The heatmaps represent the localizations in >650 cells for each strain. EzrA-YFP localization was analyzed in RH425 wild-type (**B**) and a strain where the native *cozE^{Spn}* is deleted and instead expressed from the ComS-inducible promoter P_{comX} [34]. The *cozE^{Spn}*-depletion strain (Δ*cozE^{Spn}* and P_{comX}-CozE^{Spn}) was grown with (**C**) or without (**D**) inducer peptide ComS. The arrows point to examples of cells with mislocalized EzrA-GFP. The scale bars are 2 µm.